Adsorption Behavior of Charged Zinc Porphyrins at the Water/1,2Dichloroethane Interface Studied by Potential Modulated Fluorescence Spectroscopy

ARTICLE *in* THE JOURNAL OF PHYSICAL CHEMISTRY B · JULY 2000

Impact Factor: 3.3 · DOI: 10.1021/jp001106j · Source: OAI

5 AUTHORS, INCLUDING:

Hirohisa Nagatani
Kanazawa University
51 PUBLICATIONS **696** CITATIONS
SEE PROFILE

Rodrigo Iglesias
National Scientific and Technical Research C…
29 PUBLICATIONS **468** CITATIONS
SEE PROFILE

Pierre-Francois Brevet
Claude Bernard University Lyon 1
173 PUBLICATIONS **2,830** CITATIONS
SEE PROFILE

Hubert H Girault
École Polytechnique Fédérale de Lausanne
556 PUBLICATIONS **13,980** CITATIONS
SEE PROFILE

Adsorption Behavior of Charged Zinc Porphyrins at the Water/1,2-Dichloroethane Interface Studied by Potential Modulated Fluorescence Spectroscopy

Hirohisa Nagatani,[†] Rodrigo A. Iglesias,[‡] David J. Fermín,[†] Pierre-François Brevet,[†] and Hubert H. Girault*,[†]

Laboratoire d'Electrochimie, Département de Chimie, Ecole Polytechnique Fédérale de Lausanne, CH-1015 Lausanne, Switzerland, and Departamento de Fisicoquímica, Facultad de Ciencias Químicas, Universidad Nacional de Córdoba, Córdoba 5000, Argentina

Received: March 23, 2000; In Final Form: May 17, 2000

The adsorption properties of ionic fluorescent dyes at the polarized water/1,2-dichloroethane interface were studied by potential modulated fluorescence (PMF) spectroscopy under total internal reflection. Analysis of the frequency-dependent fluorescence associated with modulation of the interfacial concentration of the ionic dyes proved to be a rather sensitive approach for separating interfacial phenomena from bulk responses. The combination of PMF and electrochemical techniques allows to uncover differences in the specific interfacial interactions of tris(2,2′-bipyridyl)ruthenium(II) ($Ru(bpy)_3^{2+}$), *meso*-tetrakis(*N*-methylpyridyl)porphyrinato zinc(II) ($ZnTMPyP^{4+}$), and *meso*-tetrakis(*p*-sulfonatophenyl)porphyrinato zinc(II) ($ZnTPPS^{4-}$). While $Ru(bpy)_3^{2+}$ shows quasi-reversible ion transfer features, the charged zinc porphyrins exhibit adsorption properties at potential close to the transfer range. The anionic $ZnTPPS^{4-}$ appears to be adsorbed at the interface at potentials more positive than the formal transfer potential. On the other hand, the spectroelectrochemical data show that $ZnTMPyP^{4+}$ is adsorbed at the interface at potentials either side of the formal transfer potential. Due to the difference in the potential dependence of the adsorption processes, PMF responses associated with interfacial accumulation from the aqueous side exhibit a different phase shift with respect to adsorption steps from the organic side. The experimental results clearly demonstrate that adsorption planes at the organic and aqueous side of the interface are physically distinguishable. Furthermore, PMF dependence on the polarization of the excitation beam allows to estimate average molecular orientation of the adsorbed species.

1. Introduction

The structure of interfaces between two immiscible electrolyte solutions (ITIES) is a rather controversial topic that has a major importance in the understanding of the mechanism involved in charge-transfer processes.[1−3] Progress toward molecular description of ionic species at the liquid−liquid interface has been achieved by surface sensitive spectroscopic techniques such as absorption−fluorescence spectroscopy under total internal reflection (TIR) conditions,[4−11] surface second harmonic generation[12−16] and quasi-elastic laser scattering.[17−19] Relevant contributions have also emerged from molecular dynamic simulations[2,20,21] and lattice-gas modeling.[22−25] However, very few attempts have been made to couple spectroscopic information with electrochemical responses.[5,26,27] The correlation between structure and reactivity certainly lies within these two experimental approaches.

The water-soluble zinc porphyrins exhibit rather interesting properties at the polarized water/1,2-dichloroethane (DCE) junction. Photoinduced heterogeneous electron transfer in the presence of a redox species in the organic phase is one of the most fascinating features of these systems.[28−32] Under potentiostatic conditions, electron transfer involving the porphyrin excited state manifests itself as photocurrent responses. The quantum yield associated with the heterogeneous quenching process appears dependent on the nature of the redox species and on the junction potential. The photoresponses are also intimately linked to the interfacial properties of the porphyrin species, i.e., "specific adsorption".[29−31] The hydrophobic analogues of these porphyrins have also shown strong affinity for liquid/liquid interfaces.[33−36]

The nature of the specific interactions between water-soluble porphyrins and the water/DCE interface remains to be understood. This phenomenon introduces complex features in voltammetric responses and significant shifts of the potential of zero charge as obtained from impedance and surface tension measurements.[29,31] In the present contribution, the potential dependent adsorption of *meso*-tetrakis(*N*-methylpyridyl)porphyrinato zinc(II) ($ZnTMPyP^{4+}$) and *meso*-tetrakis(*p*-sulfonatophenyl)-porphyrinato zinc(II) ($ZnTPPS^{4-}$) is studied by potential modulated fluorescence spectroscopy (PMF). In this approach, a sinusoidal potential modulation is superimposed to a dc bias and the fluorescence signal is measured at the frequency of modulation. The results shown here demonstrate that the spectroscopic responses arising from the interfacial region can be effectively separated from bulk signal by locking into the frequency-dependent fluorescence. Comparisons of the PMF responses between $ZnTMPyP^{4+}$ and $ZnTPPS^{4-}$, as well as tris-(2,2′-bipyridyl)ruthenium(II) ($Ru(bpy)_3^{2+}$), revealed marked difference in the adsorption properties of these dyes at the water/DCE interface. Molecular orientation and location of the adsorption plane in the case of $ZnTMPyP^{4+}$ are also discussed.

[†] Ecole Polytechnique Fédérale de Lausanne.
[‡] Universidad Nacional de Córdoba, Córdoba 5000, Argentina

10.1021/jp001106j CCC: $19.00
Published on Web 07/01/2000

Ag | Ag_2SO_4 | fluorescent 0.010 mol dm^{-3} Li_2SO_4 (aq) || 0.010 mol dm^{-3} BTPPATPFB (DCE) | 0.001 mol dm^{-3} BTPPACl 0.010 mol dm^{-3} LiCl (aq) | AgCl | Ag

Ag | Ag_2SO_4 | 0.010 mol dm^{-3} Li_2SO_4 (aq) || fluorescent 0.010 mol dm^{-3} BTPPATPFB (DCE) | 0.001 mol dm^{-3} BTPPACl 0.010 mol dm^{-3} LiCl (aq) | AgCl | Ag

Figure 1. Compositions of electrochemical cell for a fluorescent dye in an aqueous phase (upper) and an organic phase (lower).

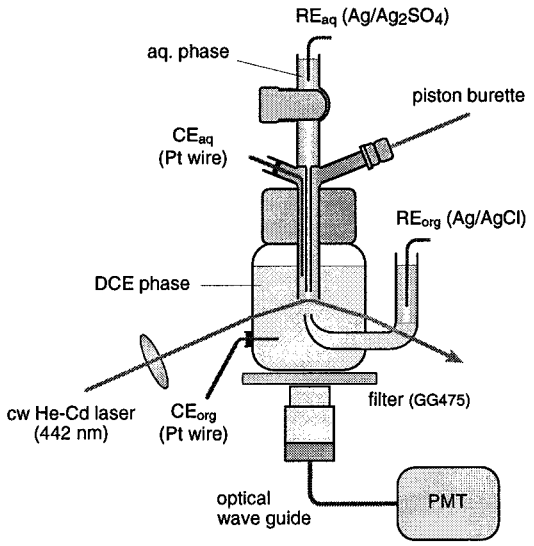

Figure 2. Schematic drawing of the optical set up in the PMF measurement.

2. Experimental Section

2.1. Reagents. All of the reagents employed were of analytical degree or higher. The organic supporting electrolyte bis(triphenylphosphoranylidene)ammonium tetrakis(pentafluorophenyl)borate (BTPPATPFB) was prepared as previously reported.[30] The *meso*-tetrakis(*N*-methyl-4-pyridyl)porphyrinato zinc(II) tetratosylate (ZnTMPyP(tos)$_4$) and *meso*-tetrakis(*p*-sulfonatophenyl)porphyrinato zinc(II) tetrasodium salt (Na_4-ZnTPPS) were purchased from Porphyrin Products. The tris(2,2′-bipyridyl)ruthenium(II) dichloride ($Ru(bpy)_3Cl_2$) was obtained from Aldrich. To dissolve $ZnTMPyP^{4+}$ into a DCE phase, the hydrophobic salt $(ZnTMPyP^{4+})(TPFB^-)_4$ was prepared by metathesis with lithium tetrakis(pentafluorophenyl)borate diethyl etharate. All aqueous solutions were prepared with highly purified water by a Milli-Q system (Millipore Milli-Q.185).

The composition of the electrolyte solutions is shown in Figure 1. These cells provide a potential window of ca. 0.6 V wide, and the Galvani potential difference ($\Delta_o^w\phi$) was estimated by taking the formal transfer potentials of tetramethylammonium (TMA^+) as 0.160 V and tetrapropylammonium (TPA^+) as −0.093 V.[37]

2.2. Apparatus and Optical Set Up. The three compartment spectroelectrochemical cell is schematically shown in Figure 2. The glass tube of 5.3 mm i.d. was filled with the aqueous phase and dipped into an organic phase (i.e., the interfacial area is 0.22 cm^2). A flat water/DCE liquid junction was formed by means of a piston buret (Metrohm E274). As displayed in Figure 2, the interface was illuminated under a TIR condition from the organic phase by a cw He−Cd laser of 132 mW at 442 nm (Omnichrome model 2074-M-A03). The critical angle for the water/DCE interface is 67.6°, and the angle of incidence for all of the studies was ca. 80°. For experiments with non-polarized laser excitation, only 15% of the laser power was employed in order to avoid bleaching of the porphyrin solution. The dependence of the PMF on the angle of light polarization was studied by placing a polarizer at the output of the laser and a rotator just before the electrochemical cell.

The water/DCE interface was polarized by a custom-made four-electrode potentiostat with a waveform generator (Hi-Tek Instruments PPR1). Platinum wires were used as counterelectrodes in both phases. The fluorescence was collected perpendicularly to the interface by a photomultiplier tube (PMT) fitted with a water-filled optical waveguide. The reflection and scattering of the incident beam were attenuated by an optical filter (GG475). The ac modulated fluorescence signal was analyzed by a lock-in-amplifier (Stanford Research Systems SR830). The potential modulation was 10 mV at the frequency of 6 Hz and the potential sweep rate was 5 mV s^{-1} unless otherwise noted.

3. Results and Discussion

3.1. Electrochemical Responses Associated with the Transfer of $Ru(bpy)_3^{2+}$, $ZnTPPS^{4-}$ and $ZnTMPyP^{4+}$. Cyclic voltammograms in the presence of the dyes of $Ru(bpy)_3^{2+}$, $ZnTPPS^{4-}$, and $ZnTMPyP^{4+}$ are displayed in Figure 3. The formal transfer potential of each species coincided, within an error margin of ca. 10 mV, with previous studies under similar experimental conditions.[31,38] The transfer response associated with $Ru(bpy)_3^{2+}$ exhibits a formal transfer potential at −0.10 V and a peak-to-peak separation of approximately 30 mV, as expected for a quasi-reversible transfer of a dicationic species.[39] More complex voltammetric responses were observed for the porphyrin complexes. In the case of $ZnTPPS^{4-}$, a well-defined transfer peak featuring a 15 mV peak-to-peak separation occurred close at −0.24 V, while a small shoulder is also observed at potentials slightly more positive. The $Ru(bpy)_3^{2+}$ and $ZnTPPS^{4-}$ transfer signals show a square root dependence on the scan rate. On the other hand, $ZnTMPyP^{4+}$ exhibits a rather more pronounced shoulder at potentials more positive than the transfer signal. These features have been associated with specific adsorption of the porphyrin complexes at the liquid/liquid junction. The dependence of the voltammetric peaks on the potential sweep rate is rather complex, suggesting the convolution of faradaic and adsorption responses.

Evidence of the interfacial accumulation of $ZnTPPS^{4-}$ and $ZnTMPyP^{4+}$ can also be seen from ac voltammetry. In Figure 4, ac voltammograms for the transfer of the three dyes are contrasted. Attenuation of the ac potential due to the uncompensated resistance was considered in the calculation of the admittance responses. The familiar bell-shaped response for the transfer of $Ru(bpy)_3^{2+}$ is centered at the formal transfer potential of the voltammetric signal displayed in Figure 3a. In the case of $ZnTPPS^{4-}$ (Figure 4b), the surface excess of this porphyrin introduces a shift of the potential of minimum imaginary admittance, indicating a displacement of the "potential of zero charge" (pzc). In the absence of $ZnTPPS^{4-}$, the minimum of the imaginary admittance is located around 0.00 V. Another interesting feature is the shoulder observed in the imaginary component of the admittance in the region between 0.20 and 0.30 V. The real part of the admittance shows a maximum at the formal transfer potential of the cyclic voltammograms at low scan rate. As discussed later, the difference between the admittance responses in Figure 4b and those obtained for $Ru(bpy)_3^{2+}$ provides evidence of not only of interfacial accumulation of $ZnTPPS^{4-}$ but also of a slow dynamics of charge transfer.

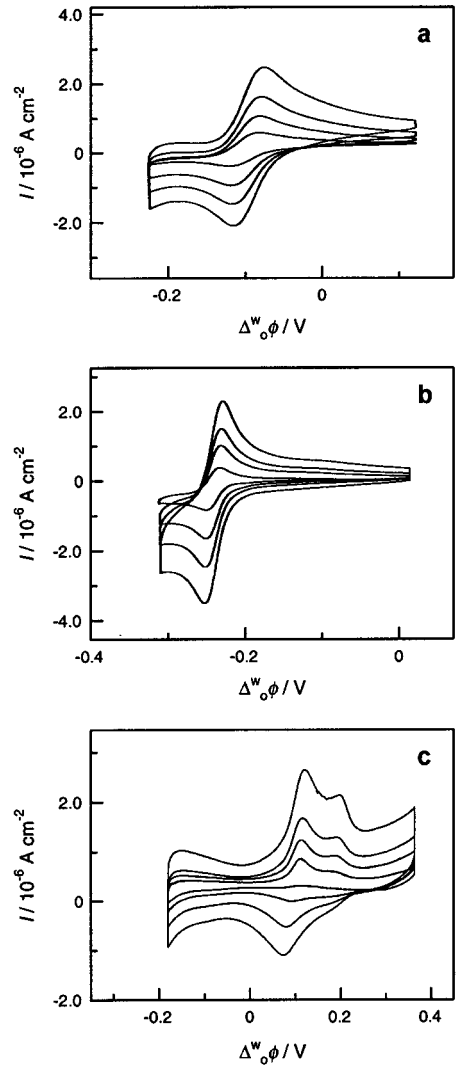

Figure 3. Cyclic voltammograms measured for $Ru(bpy)_3^{2+}$ (a), $ZnTPPS^{4-}$ (b), and $ZnTMPyP^{4+}$ (c) at 2, 5, 10, 20 mV s^{-1}. The concentration of dye in the aqueous phase was 2.5×10^{-5} mol dm^{-3}. The Galvani potential difference ($\Delta_o^w\phi$) was calibrated from the formal transfer potential of TMA^+ as 0.160 V and TPA^+ as −0.093 V.

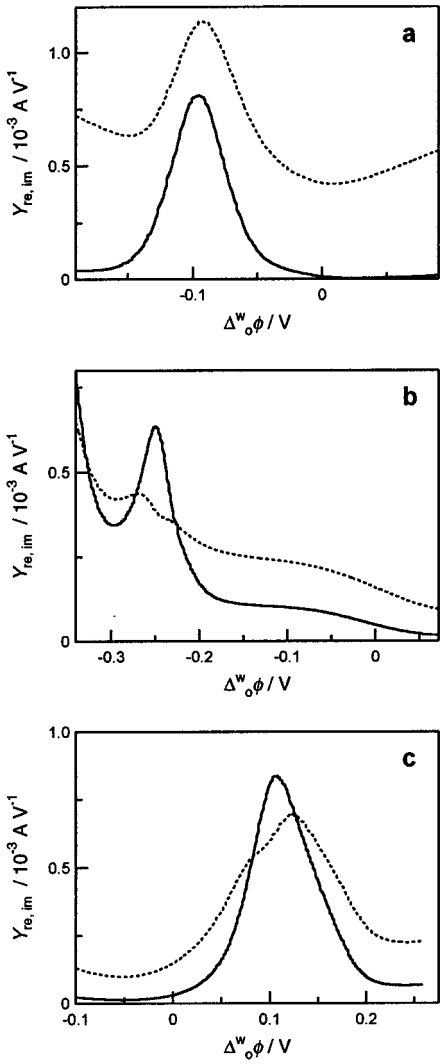

Figure 4. Real (solid line) and imaginary (dashed line) admittance measured for the ion transfer of $Ru(bpy)_3^{2+}$ (a), $ZnTPPS^{4-}$ (b), and $ZnTMPyP^{4+}$ (c). The concentration of dyes was 2.5×10^{-5} mol dm^{-3} and the potential modulation was 10 mV at 6 Hz.

The ac voltammogram of the cationic porphyrin $ZnTMPyP^{4+}$ (Figure 4c) exhibits a behavior somewhat similar to that observed for $ZnTPPS^{4-}$. The real part of the admittance features a slightly distorted bell shape, while the imaginary component shows a maximum at more positive potentials preceded by a shoulder close to 0.10 V. The potential of the maximum real part coincides with the formal transfer potential of the voltammetric response at a slow sweep rate (Figure 3c). The maximum in the imaginary part appears at 50 mV more positive than in the real component, suggesting that $ZnTMPyP^{4+}$ accumulates at the interface after it is transferred.

To gain further information on the interfacial properties of $ZnTMPyP^{4+}$, the electrochemical responses associated with the transfer from the organic to the aqueous phase were also studied. Figure 5 shows the cyclic and ac voltammograms in the presence of $(ZnTMPyP^{4+})(TPFB^-)_4$ in the DCE phase. Although the sharp voltammetric response corresponding to the porphyrin transfer appears in a similar fashion for both cases, the features at more positive potential are slightly different. The ac voltammogram in Figure 5b was obtained at a concentration 10 times more dilute than the corresponding experiment in the aqueous phase. It is clearly seen that the magnitude of the response near 0.10 V decreases with respect to the peak at more positive potentials. At higher concentrations, the ac voltammograms for the transfer from the organic phase are very similar to the curves shown in Figure 4c. This behavior further confirms that the electrochemical responses at potentials close to 0.15 V correspond to the interfacial accumulation of the porphyrin from the organic side.

3.2. Potential Modulated Fluorescence Spectroscopy of the Dye Species at the Interface. Previous fluorescence studies under the TIR condition have addressed the properties of dyes present at the liquid/liquid junction.[9,40] By modulating the Galvani potential difference across the interface and collecting the frequency-dependent fluorescence, the contribution of the species at the interface can be effectively deconvoluted from the spectroscopic signal arising from the bulk media. Consequently, this approach provides a rather powerful tool for in situ correlation of electrochemical responses and interfacial sensitive spectroscopy.

The PMF responses as a function of the Galvani potential difference in the presence $Ru(bpy)_3^{2+}$ are shown in Figure 6a. A bell-shaped response centered at −0.10 V is observed, which coincides with the ac voltammetric signal in Figure 4a. The signs of the real and imaginary components of the normalized ac fluorescence ($\Delta F/F$) are consistent with the phase shift

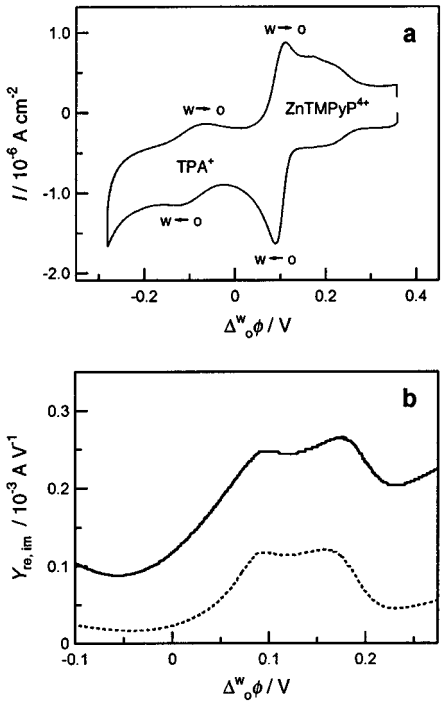

Figure 5. Cyclic voltammogram (a) and ac voltammogram (b) in the presence of $(ZnTMPyP^{4+})(TPFB^{-})_4$ in the DCE phase. The dashed and solid lines in (b) denote the real and imaginary components. The concentrations of $(ZnTMPyP^{4+})(TPFB^{-})_4$ were 2.5×10^{-5} mol dm^{-3} (a) and 2.5×10^{-6} mol dm^{-3} (b), respectively.

expected for a quasi-reversible ion transfer process.[7] Assuming a quasi-reversible ion transfer process, the real and imaginary component of $\Delta F/F$ can be estimated as described in the appendix as

$$\left(\frac{\Delta F}{F}\right)_{re} = \Theta \frac{(\Delta_o^w \phi)_1 \sigma \omega^{-1.5}}{(R_{ct} + \sigma\omega^{-0.5})^2 + (\sigma\omega^{-0.5})^2} \quad (1)$$

$$\left(\frac{\Delta F}{F}\right)_{im} = -\Theta \frac{(\Delta_o^w \phi)_1 (R_{ct} + \sigma\omega^{-0.5})\omega^{-1}}{(R_{ct} + \sigma\omega^{-0.5})^2 + (\sigma\omega^{-0.5})^2} \quad (2)$$

where Θ is the constant value which consists of the Faraday constant, the illuminated interfacial area, the charge number, and the steady-state concentration of the transferring ion. $(\Delta_o^w \phi)_1$ is the amplitude of potential modulation, R_{ct} is the charge-transfer resistance and σ is the Warburg term associated with the diffusion of the transferring ion to the interface.[7,41−43] In Figure 7, ac voltammograms are contrasted to PMF responses for various phenomenological rate constants of ion transfer. The difference in the magnitude between the real and imaginary component of $\Delta F/F$ can be associated to the value of R_{ct}. For ion transfer coefficients of the order of 1 cm s^{-1} or higher, no difference in the magnitude of both components is observed. Indeed, it appears that the difference in the magnitude of the real and imaginary part of the PMF for the $Ru(bpy)_3^{2+}$ and $ZnTPPS^{4-}$ transfer suggests that the rate constant of this process is slower than the previous limit. Although the PMF responses are not affected by the nonfaradaic responses, such as double layer charging, the spectroscopic responses are still affected by attenuation of the ac potential due to the uncompensated resistance. To assess the kinetics of ion transfer, the dependence of $\Delta F/F$ on the frequency of potential modulation should be evaluated.[7,26]

The normalized ac fluorescence in the presence of $ZnTPPS^{4-}$ exhibits additional features in comparison to the case of $Ru(bpy)_3^{2+}$ as illustrated in Figure 6b. Comparison between the ac voltammogram (Figure 4b) and the PMF (Figure 6b) revealed that the spectroscopic responses corresponding to the transfer of $ZnTPPS^{4-}$ are developed at potentials around −0.24 V. These responses feature the characteristic phase shift given by eqs 1 and 2. At potentials more positive, an additional spectroscopic signal is developed featuring a negative real part and a positive imaginary component. These responses are related to a potential-dependent excess concentration of $ZnTPPS^{4-}$ at the liquid/liquid junction, which is also connected to the shift of the pzc revealed by the ac voltammogram in Figure 4b.

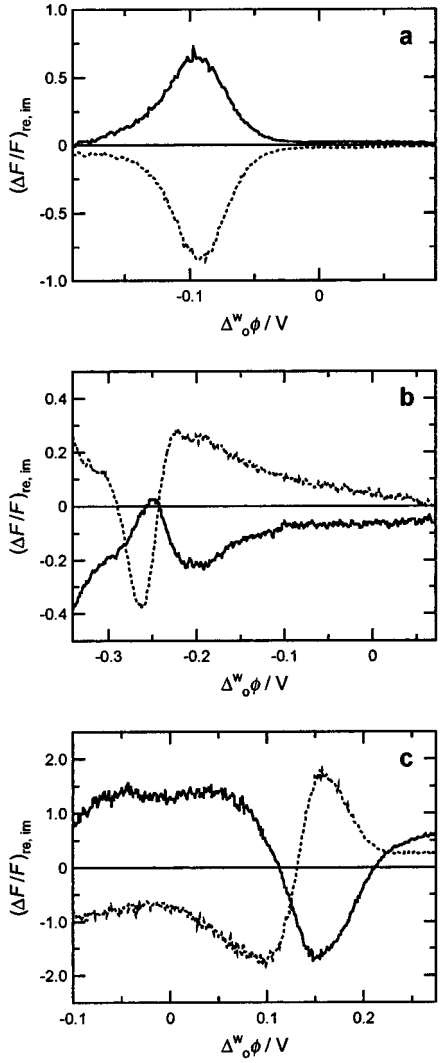

Figure 6. Typical PMF spectra for the ion transfer of $Ru(bpy)_3^{2+}$ (a), $ZnTPPS^{4-}$ (b), and $ZnTMPyP^{4+}$ (c). The solid and dashed lines denote the real and imaginary components. The concentration of dyes was 2.5×10^{-5} mol dm^{-3} and the potential modulation was 10 mV at 6 Hz.

In Figure 6c, the PMF responses in the presence of $ZnTMPyP^{4+}$ also feature a bipolar signal similar to those observed for $ZnTPPS^{4-}$. In this case, the change in the phase shift is observed at potentials more positive than the transfer response, i.e., after the transfer of the cationic porphyrin from water to DCE. This behavior is consistent with the post-transfer features observed in the ac voltammograms (Figure 4c) and cyclic voltammograms (Figure 3c). A surprising spectroscopic response also takes place at potentials prior to the transfer region, i.e., between −0.10 V to 0.00 V. By comparing Figures 4c and 6c, it appears that the PMF signal in this range is not associated with any faradaic response. These spectroscopic signals provide

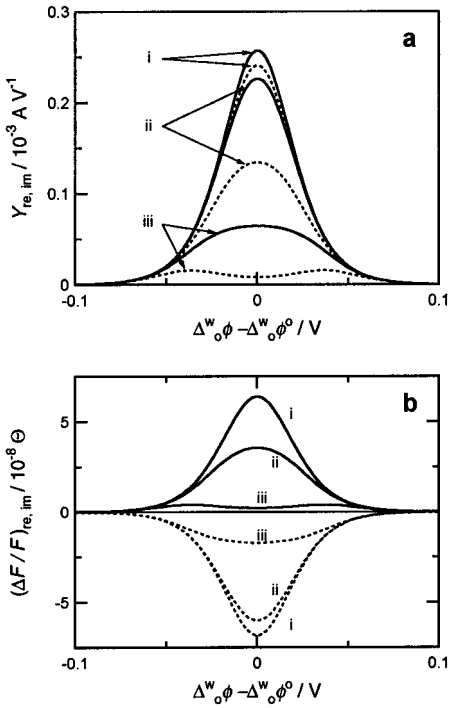

Figure 7. Numerical simulations of ac voltammogram (a) and PMF spectrum (b) for a quasi-reversible ion transfer. The solid and dashed lines denote the real and imaginary components. $\Delta^w_o\phi^\circ$ is the formal transfer potential. The ion transfer coefficient was 0.1 (i), 0.01 (ii), and 0.001 cm s^{-1} (iii). The potential modulation, the illuminated interfacial area, and the concentration and diffusion coefficients of the dicationic dye in an aqueous phase were taken as 10 mV at 6 Hz, 0.2 cm^2, 2.5×10^{-5} mol dm^{-3}, and 1×10^{-5} cm^2 s^{-1}, respectively.

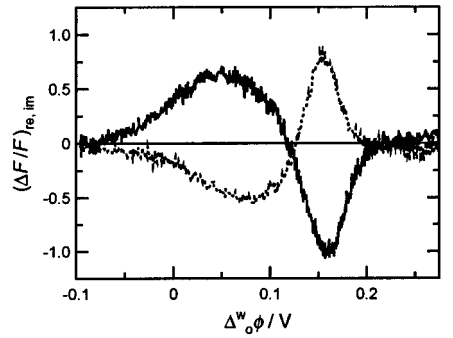

Figure 8. Typical PMF spectra measured in the presence of $(ZnTMPyP^{4+})(TPFB^-)_4$ in the DCE phase. The solid and dashed lines denote the real and imaginary components. The concentration of $(ZnTMPyP^{4+})(TPFB^-)_4$ was 2.5×10^{-6} mol dm^{-3}.

further evidence of the complex nature of the $ZnTMPyP^{4+}$ transfer mechanism.

Additional information on the behavior of $ZnTMPyP^{4+}$ was derived from PMF studies of the transfer process from DCE to water. Figure 8 displays the PMF responses associated with the transfer of the cationic porphyrin introduced in the organic phase as $(ZnTMPyP^{4+})(TPFB^-)_4$ under the same conditions as in Figure 5b. The experimental arrangement is identical to that shown in Figure 2. Despite fluorescence signal arising throughout the optical path, the results in Figure 8 demonstrate the capabilities of this technique for extracting interfacial signal, i.e., frequency-dependent responses, from those arising from the bulk. In accordance to the results in Figure 6c, the PMF responses show the interfacial accumulation of the porphyrin prior to the transfer from the organic to the aqueous phase. Under these conditions, the PMF responses qualitatively resemble the behavior observed for the transfer of $ZnTPPS^{4-}$ from water to DCE (Figure 6b).

The PMF signal in Figure 8 shows a slightly bell-shaped response at the transfer potential range of the porphyrin, i.e., between 0.00 and 0.10 V. This feature seems to contrast with the responses in Figure 6c, where the PMF responses appear at potentials as negative as −0.10 V. However, upon increasing the concentration of the $ZnTMPyP^{4+}$ in DCE, the responses at more negative potentials are clearly observed (see for instance Figure 9). This behavior further suggests that the transfer mechanism of $ZnTMPyP^{4+}$ across the water/DCE junction exhibits an interfacial accumulation both on the aqueous and the organic side.

From the results obtained for $ZnTMPyP^{4+}$, an important concept can be qualitatively rationalized concerning the physical description of adsorption planes at liquid/liquid interfaces. Considering the transfer of a cation from the aqueous to the organic phase, the potential dependent coverage will increase as $\Delta^w_o\phi$ is increased. On the other hand, if an adsorption step takes place after the transfer to the organic phase, the coverage in this plane will decrease with increasing $\Delta^w_o\phi$. Consequently, the ac fluorescence signal should undergo a 180° change in phase as the dc potential is swept from the range of adsorption at the aqueous side to the adsorption at the organic side, assuming that the adsorption dynamics are similar. The results in Figure 6c are qualitatively consistent with this interpretation, suggesting that adsorption planes on either side of the interface are physically distinguishable.

3.3. Molecular Orientation of $ZnTMPyP^{4+}$ Adsorbed at the Interface. The various PMF features associated with interfacial accumulation of porphyrins can be addressed as a function of the angle of polarization of the excitation beam (Ψ). Interfacial orientation of fluorescence probes, including $ZnTMPyP^{4+}$, has been determined by the dependence of the fluorescence intensity on Ψ.[44−47] In this section, we shall concentrate on the behavior of the cationic porphyrin. Although some dependence of the PMF responses on Ψ has been observed for $ZnTPPS^{4-}$ at potentials prior to the transfer to the organic phase; the magnitude of these responses is very small and difficult to analyze quantitatively. No dependence of the PMF signal on Ψ was observed for $Ru(bpy)_3^{2+}$, further confirming the lack of adsorption of $Ru(bpy)_3^{2+}$ at the liquid/liquid junction.

The dependence of the PMF spectrum on Ψ for the transfer of $ZnTMPyP^{4+}$ from water to DCE is illustrated in Figure 9a. A complex behavior is observed throughout the potential range, indicating that the signals associated with the interfacial accumulation and transfer are partially convoluted. In the potential range between −0.10 to 0.10 V, it is observed a decrease of the in-phase PMF response as the light polarization is varied from *s* (normal to the plane of incidence) to *p* (plane of incidence). Considering that the adsorption of porphyrin is faster than the frequency of potential modulation, it is expected that the real component of the PMF is more sensitive to the changes in the surface excess. On the other hand, the imaginary component is mostly correlated to the faradaic processes as indicated by eq 2. The behavior of the real part of the PMF suggests that the surface excess population of the porphyrin exhibits a preferential orientation. The fact that the PMF response is larger for *s*-polarization suggests that the transition dipoles are largely projected in the plane parallel to the interface. However, quantification of the orientation of the porphyrin adsorbed from the aqueous side is rather complex due to overlap with the ion transfer response. The PMF signal associated with

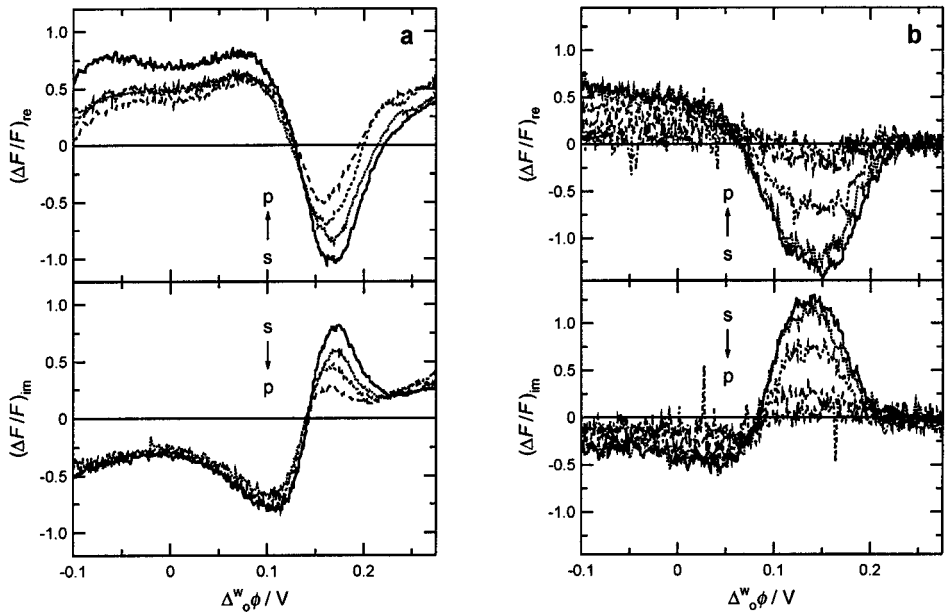

Figure 9. Dependence of PMF spectrum on the polarization of excitation beam measured for the $ZnTMPyP^{4+}$ transfer across the interface. The curves in (a) were obtained by placing the porphyrin initially in the aqueous phase (2.5×10^{-5} mol dm^{-3}), while (b) corresponds to the transfer from the organic phase (5×10^{-6} mol dm^{-3}). The angle of polarization (Ψ) was defined as the angle from the normal to the interface and varied from 90° (*s*-polarization) to 0° (*p*-polarization).

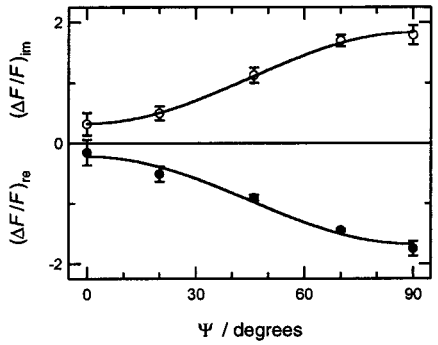

Figure 10. Polarization-dependent PMF signal at 0.15 V measured for $(ZnTMPyP^{4+})(TPFB^-)_4$. Solid lines were obtained by the least-squares curve-fitting with eq 3. The concentration of $(ZnTMPyP^{4+})$-$(TPFB^-)_4$ was 5×10^{-6} mol dm^{-3}.

the ion transfer is determined by the ac concentration of porphyrin in the organic side, and is therefore unaffected by Ψ.

The PMF responses associated with the $ZnTMPyP^{4+}$ accumulation at the organic side of the interface do show a clear dependence on the angle of polarization. The real and imaginary components developed between 0.10 and 0.20 V also decrease as Ψ is varied from *s* to *p*. This behavior is even more pronounced when the porphyrin is initially present in the DCE phase as illustrated in Figure 9b. The fact that the illumination is under the TIR condition from the DCE phase could be the reason the modulation of the surface excess charge at the organic side is the most prominent feature in Figure 9b. However, a clear dependence of the real part of the PMF signal on Ψ at negative potentials is also observed, similar to that illustrated in Figure 9a.

The fluorescence intensity at the peak of the adsorption response from the organic side (0.15 V) is displayed as a function of Ψ in Figure 10. While the PMF responses appear more weakly affected by the polarization angle when the porphyrin is initially located in the aqueous phase, a large intensity difference is observed in the reverse case. This behavior indicates a sharp distribution of the tilting angle of the adsorbed species. This dependence is related to the average orientation of the transition dipole moment of $ZnTMPyP^{4+}$. For the $\pi-\pi^*$ transition in porphyrin systems, the absorption transition dipoles, μ_1 and μ_2, and the emission transition dipoles, ν_1 and ν_2, are perpendicular to each other and parallel to the pyrrole ring (in plane).[48] Since ZnTMPyP is a highly symmetrical molecule (D_{4h}), it can be predicted that the contribution of the transition dipoles for absorption and respective emission is equal.

As the adsorption plane can be considered in the same phase of the incident beam, i.e., excitation does not involve the evanescent wave, the average tilting angle (θ) can be calculated simply by[46,49]

$$\frac{\Delta F(\Psi)}{F} = C(\sin^2\theta \cos^2(90 - \Psi) + (\cos^2\alpha \sin^2\theta + 2\sin^2\alpha \cos^2\theta) \sin^2(90 - \Psi)) \quad (3)$$

where, α and C are the angle of incidence and a proportionality value, respectively. The solid lines in Figure 10 correspond to the fits of eq 3, taking θ and C as the adjusting parameters. The value of θ was evaluated as $69 \pm 2°$ and $78 \pm 4°$ for the cases when the porphyrin was initially placed in the aqueous and organic phase, respectively. Although the dependence of the adsorption signal with the angle of polarization is quite distinctive for the cases in Figure 10, the differences in the molecular orientation are relatively small. It should also be considered that when the porphyrin is initially placed in the aqueous phase, the responses associated with the transfer to the organic phase can be partially convoluted with the adsorption signal (see Figure 9a).

The phase shift of the PMF responses associated with the adsorption processes is another aspect that remains to be solved. So far, it appears that the sign of the real and imaginary components of the PMF is related to the potential dependence of the interfacial coverage. Preliminary frequency dependence analyses of the PMF responses show a very complex dynamics in the range of 1 to 100 Hz, indicating that these processes do not correspond to a reversible ionic adsorption reaction.

4. Conclusion

The adsorption properties of fluorescence dyes at the water/DCE interface can be effectively studied by potential modulated fluorescence spectroscopy. While $Ru(bpy)_3^{2+}$ shows an apparent simple quasi-reversible transfer behavior, the porphyrins $ZnTPPS^{4-}$ and $ZnTMPyP^{4+}$ exhibit potential dependent adsorption properties. Close examination of electrochemical and spectroscopic data collected under identical conditions allow identification of the adsorption and transfer potential range. One of the fundamental ideas derived from this work is that adsorption planes can be located at the aqueous and organic side of the interface. In the case of ZnTPPS,$^{4-}$ adsorption is clearly observed at the aqueous side prior to the transfer across the interface. A relevant question in connection to the adsorption phenomena is whether the interfacial accumulation solely relies on electrostatic forces or if chemical interactions are also involved. Recent surface second harmonic studies have revealed the presence of surface excess of $ZnTPPS^{4-}$ and $ZnTMPyP^{4+}$ at the water/DCE interface even in the absence of supporting electrolyte. This result can be taken as evidence that specific adsorption of ionic species does not necessarily involve interfacial ion pairing as suggested by Cheng et al.[50,51]

In the case of $ZnTMPyP^{4+}$, PMF responses show that the porphyrin is adsorbed at the interface on both the aqueous and organic sides. The orientation of the porphyrin adsorbed at the organic side of the interface was estimated by the dependence of the PMF signal on the light polarization angle. As the porphyrin is transferred from the aqueous phase, the accumulation at the organic side was preferentially oriented with an angle of $69 \pm 2°$ with respect to the normal of the interface. When the porphyrin was initially located at the organic side, the molecules were more tilted ($78 \pm 4°$). This small difference introduced significant difference on the dependence on the polarization angle.

Interesting aspects can be introduced from comparison of the interfacial properties and the photoreactivities of the dye species toward heterogeneous photoinduced electron transfer. For instance, the photocurrent responses arising from $Ru(bpy)_2^{3+}$ sensitized water/DCE interfaces are significantly smaller than those obtained for $ZnTPPC^{4-}$ under the similar conditions.[29,31] The porphyrins, $ZnTPPS^{4-}$ and $ZnTMPyP^{4+}$, do not provide substantial photoresponses either. However, the complex ion pair $[ZnTPPS^{4-}]-[ZnTMPyP^{4+}]$ spontaneously formed in the presence of both porphyrins does exhibit remarkably high photocurrent efficiency.[31,32] As discussed previously, this heterodimer features self-assembly properties at the interface, which could be connected to the different solvation energies and adsorption properties of them.

The phase shift and amplitude of the ac fluorescence signal contain information on the nature and dynamics of the various processes involved. By analyzing the phase shift for the interfacial accumulation of $ZnTMPyP^{4+}$ and the dependence on the dc bias, it can be rationalized whether adsorption takes place at the aqueous or organic side of the interface. However, more quantitative analysis requires further understanding of the underlying physical processes linking the electrochemical responses and the interfacial accumulation of the dye. For instance, it can be envisaged that these responses correspond to the transfer of preadsorbed species across the liquid/liquid junction. In this sense, "specific adsorption" can be related to a partially re-solvated structure which features a lower transfer energy than the fully solvated dye. In subsequent reports, we shall deal with the frequency dependence of the PMF responses in order to gain further insights into the nature of the adsorption phenomena.

Acknowledgment. The Laboratoire d'Electrochimie acknowledges the fruitful collaboration with the group of Professor Ana Baruzzi of the Universidad Nacional de Córdoba. H.N. thanks a JSPS Research Fellowships for Young Scientists. R.I. acknowledges the financial support by CONICET and FOMEC Argentina. The Fond Nationale Suisse de la Recherche Scientifique is also gratefully acknowledged for the financial support through the project 20-055692.98/1. The authors are also indebted to Henrik Jensen, Zhifeng Ding, Laure Tomaszewski, Alexis Piron, and Valerie Devaud for their contributions to this work. The Laboratoire d'Electrochimie is part of the European Network ODRELLI (Organization, Dynamics and Reactivity at Liquid/Liquid Interfaces).

Appendix

Frequency Dependent Normalized Fluorescence for a Quasi-Reversible Ion Transfer Reaction. Assuming that the concentration quenching of fluorescence is negligible, the relation between the faradaic current (I^f) and the change in fluorescence under the total internal reflection condition is given by[4,7]

$$\frac{dF}{dt} = \frac{4.606\epsilon\Phi_0 I_0}{z\mathbf{F}S\cos\alpha} I^f \qquad \text{(a1)}$$

where ϵ is the molar absorptivity, Φ_0 is the fluorescence quantum yield, I_0 is the excitation photon flux, z is the charge number of transferring ion, $\mathbf{F}$ is the Faraday constant, S is the illuminated interfacial area, and α is the angle of incidence of the excitation beam. Consider a potential modulation of the form

$$\Delta_o^w\phi = (\Delta_o^w\phi)_{dc} + (\Delta_o^w\phi)_{ac} = (\Delta_o^w\phi)_0 + (\Delta_o^w\phi)_1 \exp(i\omega t) \qquad \text{(a2)}$$

The frequency-dependent fluorescence (ΔF) can be obtained following the same procedure previously reported for potential modulated reflectance[7]

$$i\omega\Delta F = \frac{4.606\epsilon\Phi_0 I_0}{z\mathbf{F}S\cos\alpha} I^f_{ac} \qquad \text{(a3)}$$

Equation a3 indicates that the ac component of the fluorescence is 90° shifted with respect to the frequency-dependent faradaic current (I^f_{ac}). It is rather more convenient to the normalized ΔF with respect to the total dc fluorescence (F), therefore, eq. a3 can be rewritten as

$$i\omega\left(\frac{\Delta F}{F}\right) = \frac{1}{z\mathbf{F}Sc_0^{org}} I^f_{ac} \qquad \text{(a4)}$$

where c_0^{org} is the steady-state concentration of the transferring dye in the organic phase.

References and Notes

(1) Samec, Z.; Marecek, V.; Homolka, D. *Faraday Discuss. Chem. Soc.* **1984**, 197.

(2) Benjamin, I. *Annu. Rev. Phys. Chem.* **1997**, *48*, 407.

(3) Fermín, D. J.; Lahtinen, R. Dynamic aspects of heterogeneous electron-transfer reactions at liquid/liquid interfaces. In *Liquid Interfaces in Chemical, Biological, and Pharmaceutical Applications*; Volkov, A., Ed.; Marcel Dekker: New York, in press.

(4) Kakiuchi, T.; Takasu, Y. *Anal. Chem.* **1994**, *66*, 1853.

(5) Kakiuchi, T.; Takasu, Y. *J. Electroanal. Chem.* **1995**, *381*, 5.

(6) Kakiuchi, T.; Takasu, Y. *J. Phys. Chem. B* **1997**, *101*, 5963.
(7) Fermín, D. J.; Ding, Z.; Brevet, P.-F.; Girault, H. H. *J. Electroanal. Chem.* **1998**, *447*, 125.
(8) Tomaszewski, L.; Ding, Z. F.; Fermín, D. J.; Cacote, H. M.; Pereira, C. M.; Silva, F.; Girault, H. H. *J. Electroanal. Chem.* **1998**, *453*, 171.
(9) Ishizaka, S.; Nakatani, K.; Habuchi, S.; Kitamura, N. *Anal. Chem.* **1999**, *71*, 419.
(10) Saitoh, Y.; Watarai, H. *Bull. Chem. Soc. Jpn.* **1997**, *70*, 351.
(11) Okumura, R.; Hinoue, T.; Watarai, H. *Anal. Sci.* **1996**, *12*, 393.
(12) Brevet, P.-F.; Girault, H. H. Second harmonic generation at liquid/liquid interfaces. In *Liquid/Liquid Interfaces: Theory and Methods*; Volkov, A. G., Ed.; CRC Press: Boca Raton, 1996; p 103.
(13) Brevet, P.-F. *Surface Second Harmonic Generation*; Presses Polytechniques Universitaires Romandes: Lausanne, 1997.
(14) Kott, K. L.; Higgins, D. A.; McMahon, R. J.; Corn, R. M. *J. Am. Chem. Soc.* **1993**, *115*, 5342.
(15) Shi, X.; Borguet, E.; Tarnovsky, A. N.; Eisenthal, K. B. *Chem. Phys.* **1996**, *205*, 167.
(16) Naujok, R. R.; Paul, H. J.; Corn, R. M. *J. Phys. Chem.* **1996**, *100*, 10497.
(17) Löfgren, H.; Neuman, R. D.; Scriven, L. E.; Davis, H. T. *J. Colloid Interface Sci.* **1984**, *98*, 175.
(18) Zhang, Z. H.; Tsuyumoto, I.; Takahashi, S.; Kitamori, T.; Sawada, T. *J. Phys. Chem. A* **1997**, *101*, 4163.
(19) Takahashi, S.; Tsuyumoto, I.; Kitamori, T.; Sawada, T. *Electrochim. Acta* **1998**, *44*, 165.
(20) Schweighofer, K. J.; Benjamin, I. *J. Electroanal. Chem.* **1995**, *391*, 1.
(21) Fernandes, P. A.; Cordeiro, M. N. D. S.; Gomes, J. A. N. F. *J. Phys. Chem. B* **1999**, *103*, 6290.
(22) Schmickler, W. *J. Electroanal. Chem.* **1997**, *428*, 123.
(23) Schmickler, W. *J. Electroanal. Chem.* **1997**, *426*, 5.
(24) Pereira, C. M.; Schmickler, W.; Silva, F.; Sousa, M. J. *J. Electroanal. Chem.* **1997**, *436*, 9.
(25) Pereira, C. M.; Schmickler, W.; Silva, A. F.; Sousa, M. J. *Chem. Phys. Lett.* **1997**, *268*, 13.
(26) Ding, Z. F.; Reymond, F.; Baumgartner, P.; Fermín, D. J.; Brevet, P. F.; Carrupt, P. A.; Girault, H. H. *Electrochim. Acta* **1998**, *44*, 3.
(27) Ding, Z.; Brevet, P.-F.; Girault, H. H. *Chem. Commun.* **1997**, 2059.
(28) Fermín, D. J.; Ding, Z.; Duong, H. D.; Brevet, P.-F.; Girault, H. H. *J. Chem. Soc., Chem. Commun.* **1998**, 1125.
(29) Fermín, D. J.; Ding, Z.; Duong, H.; Brevet, P.-F.; Girault, H. H. *J. Phys. Chem. B* **1998**, *102*, 10334.
(30) Fermín, D. J.; Duong, H.; Ding, Z.; Brevet, P.-F.; Girault, H. H. *Phys. Chem. Chem. Phys.* **1999**, *1*, 1461.
(31) Fermín, D. J.; Duong, H.; Ding, Z.; Brevet, P.-F.; Girault, H. H. *J. Am. Chem. Soc.* **1999**, *121*, 10203.
(32) Fermín, D. J.; Doung, H.; Ding, Z.; Brevet, P.-F.; Girault, H. H. *Electrochem. Commun.* **1999**, *1*, 29.
(33) Nagatani, H.; Watarai, H. *J. Chem. Soc., Faraday Trans.* **1998**, *94*, 247.
(34) Nagatani, H.; Watarai, H. *Chem. Lett.* **1997**, 167.
(35) Nagatani, H.; Watarai, H. *Anal. Chem.* **1998**, *70*, 2860.
(36) Nagatani, H.; Watarai, H. *Chem. Lett.* **1999**, 701.
(37) Girault, H. H. See the web site dcwww.epfl.ch for a comprehensive list of free energy of ion transfer at various liquid/liquid interfaces.
(38) Ding, Z. F.; Wellington, R. G.; Brevet, P.-F.; Girault, H. H. *J. Phys. Chem.* **1996**, *100*, 10658.
(39) Samec, Z.; Homolka, D.; Marecek, V.; Kavan, L. *J. Electroanal. Chem.* **1983**, *145*, 213.
(40) Ishizaka, S.; Habuchi, S.; Kim, H. B.; Kitamura, N. *Anal. Chem.* **1999**, *71*, 3382.
(41) Osakai, T.; Kakutani, T.; Senda, M. *Bull. Chem. Soc. Jpn.* **1984**, *57*, 370.
(42) Osakai, T.; Kakutani, T.; Senda, M. *Bull. Chem. Soc. Jpn.* **1985**, *58*, 2626.
(43) Wandlowski, T.; Marecek, V.; Samec, Z. *J. Electroanal. Chem.* **1988**, *242*, 291.
(44) Bos, M. A.; Kleijn, J. M. *Biophys. J.* **1995**, *68*, 2566.
(45) Bos, M. A.; Kleijn, J. M. *Biophys. J.* **1995**, *68*, 2573.
(46) Ohta, N.; Matsunami, S.; Okazaki, S.; Yamazaki, I. *Langmuir* **1994**, *10*, 3909.
(47) Azumi, R.; Matsumoto, M.; Kawabata, Y.; Kuroda, S.; Sugi, M.; King, L. G.; Crossley, M. J. *J. Phys. Chem.* **1993**, *97*, 12862.
(48) Gouterman, M. *The Porphyrins*; Dolphin, D., Ed.; Academic Press: New York, 1978; Vol. III.
(49) Akutsu, H.; Kyogoku, Y.; Nakahara, H.; Fukuda, K. *Chem. Phys. Lipids* **1975**, *15*, 222.
(50) Cheng, Y.; Cunnane, V. J.; Schiffrin, D. J.; Murtomaki, L.; Kontturi, K. *J. Chem. Soc., Faraday Trans.* **1991**, *87*, 107.
(51) Cheng, Y.; Schiffrin, D. J. *J. Chem. Soc., Faraday Trans.* **1993**, *89*, 199.